Data consistency networks for (calibration-less) accelerated parallel MR image reconstruction
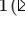
Jo Schlemper[1]([✉]), Jinming Duan[1], Cheng Ouyang[1], Chen Qin[1], Jose Caballero[1],
Joseph V. Hajnal[2], and Daniel Rueckert[1]

[1] Biomedical Image Analysis Group, Imperial College London, UK
{jo.schlemper11,d.rueckert}@imperial.ac.uk
[2] Imaging and Biomedical Engineering Clinical Academic Group, King's College London, UK
{jo.hajnal}@kcl.ac.uk

Abstract. We present simple reconstruction networks for multi-coil data by extending deep cascade of CNNs and exploiting the data consistency layer. In particular, we propose two variants, where one is inspired by POCSENSE and the other is calibration-less. We show that the proposed approaches are competitive relative to the state-of-the-art both quantitatively and qualitatively.

1 Introduction

Recently, several deep learning approaches have been proposed for accelerated parallel MR image reconstruction[4, 6, 5, 2, 1, 11]. In this work, we present simple reconstruction networks for multi-coil data by extending deep cascade of CNNs[9]. In particular, we propose two approaches, where one is inspired by POCSENSE[8] and the other is calibration-less. The method is evaluated using a public knee dataset containing 100 subjects[4]. We show that the proposed approaches are competitive relative to the state of the art both quantitatively and qualitatively.

2 Methods

The proposed networks are direct extensions of deep cascades of CNN (DC-CNN), where the denoising sub-networks and the data consistency layers are interleaved. However, for parallel imaging, the data consistency layer can be extended in two ways, yielding two network variants. In the first approach, sensitivity estimates are required, which can be computed using algorithms such as E-SPIRiT[10]. The input to the CNN is a single, sensitivity-weighted recombined image. At each iteration, the CNN updates an estimate of the combined image. For the data
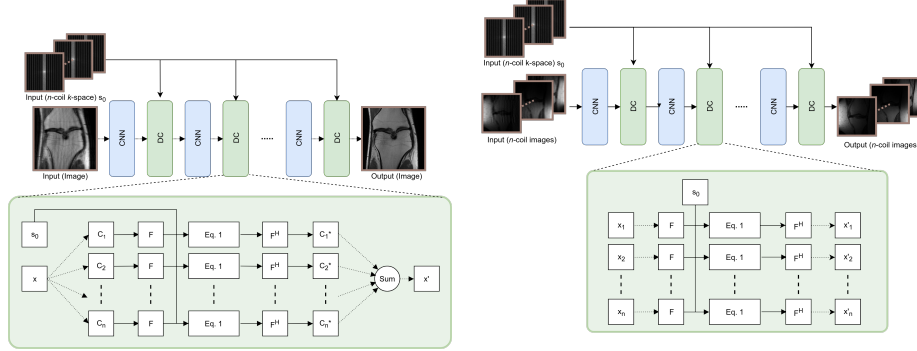

Fig. 1. The proposed network architectures. (left) D-POCSENSE architecture. The input to the CNN is a single, sensitivity-weighted recombined image. At each iteration, the CNN updates an estimate of the combined image. The sub-network takes a single recombined image as an input and produces the denoised result as an output. The data consistency is performed by mapping the intermediate output to the raw k-space by applying encoding matrix. The updated image is recombined by the adjoint of the encoding matrix. (right) The proposed DC-CNN architecture. The network jointly reconstructs each coil data simultaneously. The data consistency operation is applied separately for each coil.

consistency layer, the forward operation is performed, then acquired samples are filled coil-wise as:

$$
s_{\mathrm{rec}}^{(i)}(k) = \begin{cases} \lambda s_{\mathrm{cnn}}^{(i)}(k) + (1 - \lambda) s_0^{(i)}(k) & \text{if } k \in \Omega \\ s_{\mathrm{cnn}}^{(i)}(k) & \text{if } k \notin \Omega \end{cases} \tag{1}
$$

where $s_{\mathrm{cnn}}^{(i)}$, $s_0^{(i)}$ are the i-th coil-weighted image for the intermediate CNN reconstruction in k-space and the original k-space data respectively. The result is mapped back to image domain via the adjoint of the encoding matrix. As the operation in the data consistency layer is analogous to the projection step from POCSENSE, the proposed network is termed D(eep)-POCSENSE. The balancing term λ depends on the input noise level, however, this is made trainable as a network parameter. The network is trained using ℓ_2 loss:

$$
\ell_2(\theta) = \sum_{(x_u, x) \in D} \| x - f_{\mathrm{cnn}}(x_u; \theta) \|_2^2 \tag{2}
$$

where x_u and x are the initial recombined image and ground truth respectively.

The second approach reconstructs the multiple coil data directly without performing the recombination and the coil images are stacked along the channel-axis and fed into each sub-network. For the data consistency layer, each coil image is Fourier transformed and Eq. (1) is applied individually. As it does not require a sensitivity estimate, the proposed approach is calibration-less. The
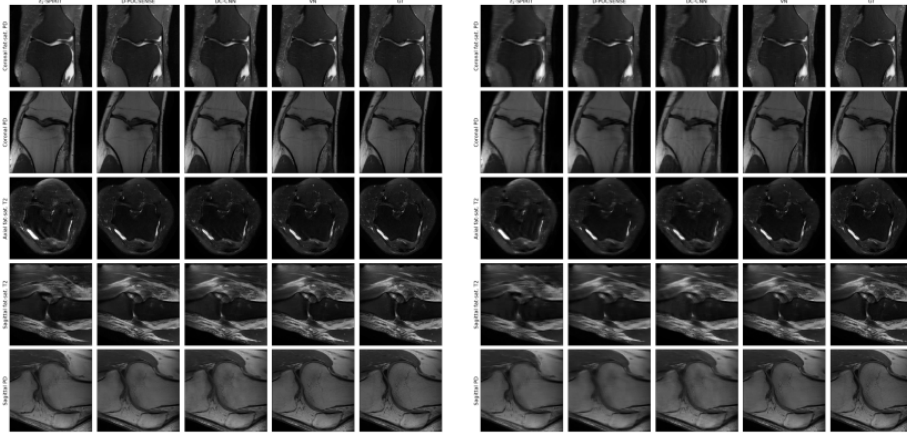
Fig. 2. (left) The reconstruction results from each method for Cartesian undersampling (left) with acceleration factor 4 and (right) acceleration factor 6.

proposed network, DC-CNN, is trained with the following weighted-ℓ_2 loss:

$$\ell_2(\theta) = \sum_{(x_u,x)\in D} \sum_{i=1}^{n_{\text{coil}}} \| C_i^H \left(x_i - f_{\text{cnn}}(x_{u,1},\ldots,x_{u,n_{\text{coil}}};\theta)_i \right) \|_2^2 \tag{3}$$

where the subscript indexes i-th coil data and C_*^H is the sensitivity map. The proposed architectures are shown in Fig. 1.

3   Evaluation

We used the public knee dataset provided by Hammernik et al.[4][3]. The dataset contains 100 patients, 20 subjects per acquisition protocol. For each approach, one network was trained to reconstruct all acquisition protocols simultaneously. We used 15 for training and 5 for testing per protocol. The proposed approach was compared with ℓ_1-SPIRiT[7] and Variational Network (VN)[4]. We used Cartesian undersampling with acceleration factor (AF) $\in \{4, 6\}$, sampling 24 central region, which was also used as the calibration region for estimating the sensitivity maps. In this work, D-POCSENSE and DC-CNN were trained with $n_{\text{coil}} = 15, n_d = 5, n_c = 10$[9] and convolution kernels with dilation factor 2. The network was trained using Adam with $lr = 10^{-3}$ for 200 epoch with batch size 4. The default parameters were used for both ℓ_1-SPIRiT and VN. We used PSNR and SSIM for the metric.

---

[3] Available at `mridata.org`.

Table 1. The summary of quantitative results for AF=4 and AF=6. PD denotes proton tensity and FS denotes fat saturation.

Modality	Model	AF=4		AF=6	
		PSNR	SSIM	PSNR	SSIM
Axial T_2 FS	ℓ_1-SPIRIT	33.55±12.62	0.87±0.26	26.61±12.83	0.80±0.30
	D-POCSENSE	36.03±10.26	0.90±0.24	31.83±8.79	**0.87±0.25**
	DC-CNN	35.45±8.63	**0.91±0.19**	30.14±6.85	**0.87±0.23**
	VN	**36.49±10.41**	0.90±0.23	**32.39±9.94**	0.86±0.29
Coronal PD	ℓ_1-SPIRIT	36.96±1.28	**0.98±0.00**	31.84±1.32	**0.95±0.01**
	D-POCSENSE	36.94±1.24	**0.98±0.00**	32.27±0.83	**0.95±0.00**
	DC-CNN	35.14±1.26	0.97±0.01	29.88±1.72	0.94±0.01
	VN	**37.07±1.15**	**0.98±0.00**	**33.17±1.06**	**0.95±0.01**
Coronal PDFS	ℓ_1-SPIRIT	36.98±7.85	0.97±0.06	33.32±6.84	0.95±0.07
	D-POCSENSE	39.02±3.37	**0.98±0.02**	34.91±2.7	**0.97±0.04**
	DC-CNN	38.37±3.23	**0.98±0.03**	33.61±2.74	0.96±0.05
	VN	**39.39±3.32**	**0.98±0.02**	**35.71±2.80**	**0.97±0.02**
Sagittal PD	ℓ_1-SPIRIT	36.76±0.47	**0.98±0.00**	31.43±0.84	0.94±0.01
	D-POCSENSE	37.09±0.54	**0.98±0.00**	31.94±0.45	0.94±0,00
	DC-CNN	35.76±0.59	0.97±0.00	30.12±1.31	0.94±0.01
	VN	**37.47±0.55**	**0.98±0.00**	**32.86±0.59**	**0.95±0.00**
Sagittal T_2 FS	ℓ_1-SPIRIT	37.71±1.55	**0.98±0.00**	33.32±1.29	**0.96±0.01**
	D-POCSENSE	37.96±1.08	**0.98±0.01**	33.43±1.08	**0.96±0.01**
	DC-CNN	37.02±1.55	**0.98±0.01**	27.76±3.04	0.95±0,01
	VN	**38.39±1.21**	**0.98±0.01**	**34.32±1.12**	**0.96±0.01**

4   Results

Quantitative results are summarised in Table 1 for each acquisition protocol. The proposed methods both outperformed the compressed sensing approach on average. D-POCSENSE achieved the performance close to VN for AF=4, whereas DC-CNN was slightly worse. All methods provided similar SSIM. For AF=6, VN achieved the highest PSNR. The sample reconstructions are shown in Fig. 2 for AF=4 and AF=6 respectively. For Axial T_2 image, D-POCSENSE gave the most homogeneous image, whereas DC-CNN and VN often failed to remove aliasing. For AF=4, all methods generated sharp images. For AF=6, DC-CNN performed worse that D-POCSENSE and VN and the residual aliasing is prominent.

5   Discussion and Conclusion

In this work, we proposed simple extensions to DC-CNN for parallel imaging. When comparing the two approaches so far explored, D-POCSENSE outperformed DC-CNN overall, which leads to the conclusion that incorporating the sensitivity

estimate is advantageous. We speculate that this is because it allows intermediate sub-networks to directly operate in the output space as well as directly optimising the loss with respect to the final output. Nevertheless, DC-CNN achieved the highest SSIM in some regimes, which shows that a novel way of combining the raw data could lead to improved algorithms. The proposed methods achieved comparable performance to state-of-the-art algorithms, however, we note that the variational network produced the best result overall.

6   Note

We observed that training D-POCSENSE and DC-CNN networks longer can further remove the residual aliasing present in the reconstruction to eventually reach similar performances. The presented work is now extended to *variable-splitting network* [3].

7   Acknowledgements

References

[1] Akçakaya, M., Moeller, S., Weingärtner, S., Uğurbil, K.: Scan-specific robust artificial-neural-networks for k-space interpolation (raki) reconstruction: Database-free deep learning for fast imaging. Magnetic resonance in medicine 81(1), 439–453 (2019)

[2] Cheng, J.Y., Mardani, M., Alley, M.T., Pauly, J.M., Vasanawala, S.S.: Deepspirit: Generalized parallel imaging using deep convolutional neural networks. ISMRM 26th Annual Meeting & Exhibition (2018)

[3] Duan, J., Schlemper, J., Qin, C., Ouyang, C., Bai, W., Biffi, C., Bello, G., Statton, B., O'Regan, D.P., Rueckert, D.: Vs-net: Variable splitting network for accelerated parallel mri reconstruction. arXiv preprint arXiv:1907.10033 (2019)

[4] Hammernik, K., Klatzer, T., Kobler, E., Recht, M.P., Sodickson, D.K., Pock, T., Knoll, F.: Learning a variational network for reconstruction of accelerated mri data. Magnetic resonance in medicine 79(6), 3055–3071 (2018)

[5] Han, Y., Sunwoo, L., Ye, J.C.: k-space deep learning for accelerated mri. IEEE transactions on medical imaging (2019)

[6] Mardani, M., Gong, E., Cheng, J.Y., Vasanawala, S.S., Zaharchuk, G., Xing, L., Pauly, J.M.: Deep generative adversarial neural networks for compressive sensing mri. IEEE transactions on medical imaging 38(1), 167–179 (2018)

[7] Murphy, M., Alley, M., Demmel, J., Keutzer, K., Vasanawala, S., Lustig, M.: Fast ell_1-spirit compressed sensing parallel imaging mri: Scalable parallel implementation and clinically feasible runtime. IEEE transactions on medical imaging 31(6), 1250–1262 (2012)

[8] Samsonov, A.A., Kholmovski, E.G., Parker, D.L., Johnson, C.R.: Pocsense: Pocs-based reconstruction for sensitivity encoded magnetic resonance imaging. Magnetic Resonance in Medicine: An Official Journal of the International Society for Magnetic Resonance in Medicine 52(6), 1397–1406 (2004)

[9] Schlemper, J., Caballero, J., Hajnal, J.V., Price, A.N., Rueckert, D.: A deep cascade of convolutional neural networks for dynamic mr image reconstruction. IEEE transactions on Medical Imaging 37(2), 491–503 (2017)

[10] Uecker, M., Lai, P., Murphy, M.J., Virtue, P., Elad, M., Pauly, J.M., Vasanawala, S.S., Lustig, M.: Espiritan eigenvalue approach to autocalibrating parallel mri: where sense meets grappa. Magnetic resonance in medicine 71(3), 990–1001 (2014)

[11] Zhang, P., Wang, F., Xu, W., Li, Y.: Multi-channel generative adversarial network for parallel magnetic resonance image reconstruction in k-space. In: International Conference on Medical Image Computing and Computer-Assisted Intervention. pp. 180–188. Springer (2018)